

## XI. SCHWARZSCHILD BLACK HOLES

We noted in Handout IX that the Schwarzschild metric is singular at  $r = 2\mu$  (and also at  $r = 0$ ).

So far, we have been concerned with motion in the region  $r > 2\mu$ , but what should we make of the region  $r < 2\mu$  and the hypersurface  $r = 2\mu$ ?

In this topic, we discuss the causal structure of the Schwarzschild solution.

We shall show that the region  $r < 2\mu$  represents a *black hole* – a region of spacetime from which no particle can escape to spatial infinity.

Moreover, we shall show that the surface  $r = 2\mu$ , while being perfectly regular, does have important physical significance as an *event horizon*.

To uncover these global properties of the Schwarzschild solution, we shall have to introduce new coordinates that allow us to join the regions  $r < 2\mu$  and  $r > 2\mu$  in a continuous manner.

### 1 Singularities in the Schwarzschild metric

The Schwarzschild line element is

$$ds^2 = c^2 \left(1 - \frac{2\mu}{r}\right) dt^2 - \left(1 - \frac{2\mu}{r}\right)^{-1} dr^2 - r^2 d\Omega^2, \quad (1)$$

where, recall,  $\mu \equiv GM/c^2$ .

The metric is singular at  $r = 0$  and at  $r = 2\mu$ .

The latter is generally called the *Schwarzschild radius*

$$r_s = 2\mu = \frac{2GM}{c^2}. \quad (2)$$

The Schwarzschild solution is a vacuum solution of the Einstein field equations, so only holds down to the surface of the spherical massive body.

If the radius of the body exceeds  $r_s$ , the singularities in the Schwarzschild solution are of no consequence (the spacetime inside the body is described by some non-vacuum solution of the field equations).

For example, for the Sun,  $r_s \approx 3$  km but the Solar radius  $R_\odot = 7 \times 10^5$  km  $\gg r_s$ .

However, if the central body is so compact that it is smaller than its Schwarzschild radius, we must take (part of) the region  $r < 2\mu$  seriously.

To investigate the nature of the singularities at  $r = 0$  and  $r = 2\mu$  we should consider coordinate-independent properties of spacetime there.

Invariants formed from the Riemann curvature tensor are suitable candidates.

Since  $R_{\mu\nu} = 0$  by construction, the first non-trivial invariant to consider is

$$R_{\mu\nu\rho\sigma}R^{\mu\nu\rho\sigma} \propto \frac{\mu^2}{r^6}. \quad (3)$$

This scalar (called the *Kretschmann scalar*) is telling us something about the magnitude of tidal effects; it has the same dependence on  $M$  and  $r$  as the square of the tidal tensor in Newtonian gravity.

We see that the Kretschmann scalar is regular at  $r = 2\mu$  but singular at  $r = 0$ .

The apparent singularity in the metric at  $r = 2\mu$  is just an artefact of our particular choice of coordinate system and so is a *coordinate singularity*.

It can be removed by adopting different coordinates (as we show later).

However, the curvature of spacetime is infinite at  $r = 0$  so this is a genuine intrinsic singularity.

---

*Example: coordinate singularities for the 2-sphere*

In Handout II, we considered the 2-sphere described in cylindrical coordinates  $(\rho, \phi)$ , for which the line element is

$$ds^2 = \frac{a^2 d\rho^2}{(a^2 - \rho^2)} + \rho^2 d\phi^2, \quad (4)$$

where  $a$  is the radius of the sphere.

The coordinate ranges are  $0 \leq \rho \leq a$  and  $0 \leq \phi < 2\pi$  and these cover just one hemisphere.

The metric is singular at  $\rho = a$ , but we know the 2-sphere is perfectly regular everywhere with nothing odd happening at the equator.

The curvature invariants are all regular (and actually are the same everywhere) as is necessary for  $\rho = a$  to be only a coordinate singularity.

---

The region  $r < 2\mu$  of the Schwarzschild solution has some very odd properties.

Let us denote the region of spacetime with  $r > 2\mu$  as *region I* and  $r < 2\mu$  as *region II*.

In region I, the coordinate basis vector  $\mathbf{e}_0 \equiv \partial/\partial t$  is timelike,

$$\mathbf{g}(\mathbf{e}_0, \mathbf{e}_0) = g_{00} = c^2 \left( 1 - \frac{2\mu}{r} \right) > 0. \quad (5)$$

This means that a curve at constant  $(r, \theta, \phi)$  is timelike.

Also, in region I the spatial basis vectors are spacelike.

However, in region II the  $\mathbf{e}_0$  basis vector is spacelike since  $g_{00} < 0$ .

Moreover, the basis vector  $\partial/\partial_r$  is timelike!

This means that a particle cannot stay at fixed  $(r, \theta, \phi)$  in region II, no matter what they do, as their worldline would then be spacelike rather than timelike.

It is as if the time and radial coordinates swap characters for  $r < 2\mu$ .

## 2 Causal structure

As timelike curves travel inside the lightcone, and null curves on the lightcone, the lightcones display the causal structure of spacetime (i.e., which events can influence others).

We can construct the lightcones in Schwarzschild spacetime by considering radial null geodesics.

### 2.1 Radial null geodesics

Radial geodesics have  $d\theta = d\phi = 0$ .

For null geodesics, it follows that

$$\begin{aligned}
 0 &= ds^2 = c^2 \left(1 - \frac{2\mu}{r}\right) dt^2 - \left(1 - \frac{2\mu}{r}\right)^{-1} dr^2 \\
 \Rightarrow \quad \frac{d(ct)}{dr} &= \pm \left(1 - \frac{2\mu}{r}\right)^{-1}.
 \end{aligned} \tag{6}$$

With the  $+$  sign, this is solved by

$$ct = r + 2\mu \ln \left| \frac{r}{2\mu} - 1 \right| + \text{const.}, \quad (7)$$

where the absolute value means we can consider both  $r > 2\mu$  and  $r < 2\mu$ .

In region  $I$ , these are a family of *outgoing* radial null geodesics.

With the  $-$  sign, Eq. (6) is solved by

$$ct = -r - 2\mu \ln \left| \frac{r}{2\mu} - 1 \right| + \text{const.} \quad (8)$$

In region  $I$ , these are a family of *ingoing* radial null geodesics.

Note the ingoing and outgoing solutions are related by time reversal,  $t \rightarrow -t$ .

(Since the Schwarzschild metric is symmetric under time reversal, the time reverse of a solution of the geodesic equations will also be a solution.)

These paths of radial null geodesics are plotted in Fig. 1 along with the lightcones that they generate.

The main features in region I are as follows.

- For  $r \gg 2\mu$ , the radial null geodesics are straight lines in the  $r$ - $ct$  plane with gradient  $\pm 1$ , corresponding to the usual lightcones in Minkowski space.
- As  $r \rightarrow 2\mu$ , the lightcones are squashed in the radial direction.
- It *seems* to take an infinite coordinate time for an ingoing photon to reach  $r = 2\mu$ .

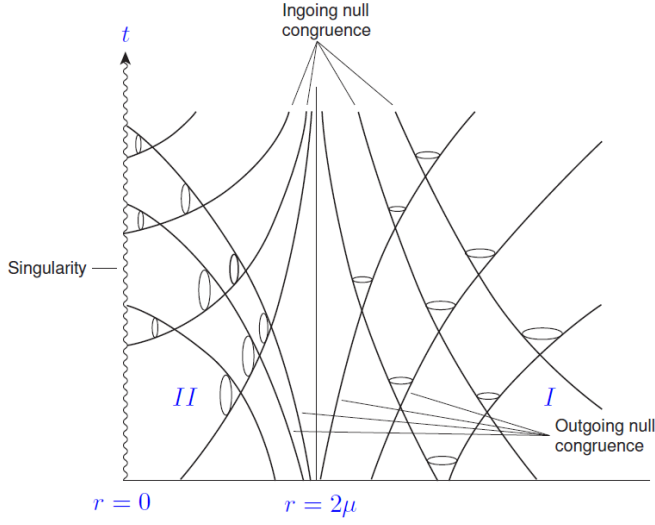


Figure 1: Lightcone structure of the Schwarzschild solution. Ingoing and outgoing radial null geodesics are shown in the  $(t, r)$  plane. Both are discontinuous at the Schwarzschild radius  $r = 2\mu$ .

- Similarly, all outgoing rays seem to originate from  $r = 2\mu$  and  $ct \rightarrow -\infty$ .

The behaviour as  $r \rightarrow 2\mu$  is misleading since an ingoing photon actually needs only a finite change in its affine parameter to cross  $r = 2\mu$ .

To see this, recall from the geodesic equations that

$$\frac{dt}{d\lambda} = k \left(1 - \frac{2\mu}{r}\right)^{-1}, \quad (9)$$

where  $\lambda$  is an affine parameter.

It follows that

$$\frac{dr}{d\lambda} = k \frac{dr}{dt} \left(1 - \frac{2\mu}{r}\right)^{-1} = \pm kc, \quad (10)$$

so that

$$r = \pm ck\lambda + \text{const.} \quad (11)$$

We see that an ingoing photon reaches  $r = 2\mu$  from some  $r_0 > 2\mu$  for a finite increment in the affine parameter.

What happens when the photon gets to  $r = 2\mu$ ?

Equation (11) tells us that the photon passes straight through continuing to the singularity at  $r = 0$  as  $\lambda$  increases further.

Moreover, since  $k > 0$ , Eq. (9) implies that  $dt/d\lambda < 0$  in region II.

We thus see that future-directed ingoing null geodesics in region I reach  $r = 2\mu$  and  $t = \infty$  at a finite value of their affine parameter, and then extend into region II moving towards  $r = 0$  with decreasing  $t$ !

It is worth pausing to restate what we have achieved here: region I (for  $r \neq 0$ ) and region II are spherically-symmetric vacuum solutions of the Einstein field equations, each covering part of spacetime, but because of the coordinate singularity it is not immediately clear how these fit together.

By extending ingoing null geodesics from region I, we see that the causal future of this region of the Schwarzschild solution includes a type-II region in which the forward lightcone is tipped over towards  $r = 0$ .

Any particle that falls into this type-II region will inevitably fall towards the singularity at  $r = 0$  *no matter what they do to try and avoid it*.

The hypersurface  $r = 2\mu$  is an example of an *event horizon* – the outermost boundary of a region of spacetime from which no particle can escape to spatial infinity.

The region II in the causal future of region I is a *black hole* – a region of spacetime from which no particle can escape to spatial infinity.

The event horizon acts like a one-way membrane, particles can fall through it from  $r > 2\mu$  to  $r < 2\mu$ , but not the other way around.

We shall shortly construct a non-singular coordinate system (*ingoing Eddington–Finkelstein coordinates*) that covers both region I and the region II in its causal future.

### 2.1.1 The causal past of region I

What if we had considered outgoing null geodesics instead in region I?

These seem to emerge from  $r = 2\mu$  at  $t = -\infty$ , but, actually, the affine parameter changes by a finite amount in travelling from  $r = 2\mu$  to some  $r_0 > 2\mu$ .

If we try and extend such outgoing geodesics back to smaller values of the affine parameter  $\lambda$ , we find that they join onto geodesics in region II that have  $r$  increasing with  $\lambda$  and  $t$  decreasing.

This is a type-II region, but it cannot be the same as that in the causal future of region I since the forward lightcone is now directed away from  $r = 0$ .

Such a region is a *white hole* in which particles are inevitably expelled to  $r > 2\mu$ !

The original Schwarzschild solution, with its single regions I and II separated by a coordinate singularity, do not cover the entire spacetime.

Rather, it can be shown that the entire spacetime contains a black hole, a white hole and *two* type-I regions.

It is possible to construct coordinates that cover all of these regions in a non-singular manner (look up *Kruskal–*



*Szekeres* coordinates).

However, the existence of white holes as a physical reality is very doubtful.

Black holes can form as the result of gravitational collapse, but white holes require the singularity to exist in the past.

## 2.2 Radially-infalling particles

We can repeat the analysis above for the timelike world-lines of massive infalling particles.

For such particles, setting  $h = 0$  in their radial effective potential, we have

$$\frac{1}{2}\dot{r}^2 - \frac{GM}{r} = \frac{1}{2}c^2(k^2 - 1), \quad (12)$$

where overdots denote differentiation with respect to proper time.

Recall also that  $\dot{t}(1 - 2\mu/r) = k$ .

Taking a further time derivative of Eq. (12) gives

$$\ddot{r} = -\frac{GM}{r^2}, \quad (13)$$

which has exactly the same form as the Newtonian equation of motion (but the time variable and  $r$  mean different things).

Consider a particle that starts at rest at infinity, so that  $k = 1$ .

For an in-falling particle,

$$\dot{r} = -\sqrt{\frac{2\mu c^2}{r}}, \quad (14)$$

so that

$$c(\tau - \tau_0) = \frac{2}{3} \left[ \left( \frac{r_0^3}{2\mu} \right)^{1/2} - \left( \frac{r^3}{2\mu} \right)^{1/2} \right], \quad (15)$$

where we have taken  $r(\tau_0) = r_0$ .

This gives us the proper time as a function of  $r$ .

It takes finite amounts of proper time to reach  $r = 2\mu$  and  $r = 0$ .

We can also determine coordinate time  $t$  as a function of  $r$  using

$$\frac{d(ct)}{dr} = \frac{c\dot{t}}{\dot{r}} = -\sqrt{\frac{r}{2\mu}} \left( 1 - \frac{2\mu}{r} \right)^{-1}. \quad (16)$$

The solution of this is

$$\begin{aligned} c(t - t_0) &= -2\mu \int_{r_0/(2\mu)}^{r/(2\mu)} \frac{x^{3/2}}{x - 1} dx \\ &= -2\mu \left[ \frac{2}{3} x^{3/2} + 2\sqrt{x} + \ln \left| \frac{\sqrt{x} - 1}{\sqrt{x} + 1} \right| \right]_{r_0/(2\mu)}^{r/(2\mu)}, \end{aligned} \quad (17)$$

where we have taken  $t(r_0) = t_0$ .

The integral is improper as  $r \rightarrow 2\mu$  and diverges logarithmically, so that  $t \rightarrow \infty$  as  $r \rightarrow 2\mu$ .

For smaller  $r$ , coordinate time then decreases with increasing  $\tau$ .

The resulting worldline is plotted in Fig. 2 for a particle with  $\tau_0 = 0$ ,  $r_0 = 8\mu$  and  $t_0 = 0$ .

Consider the in-falling particle as observed by a stationary observer at  $r = \infty$ .

Light from the particle only reaches the distant observer

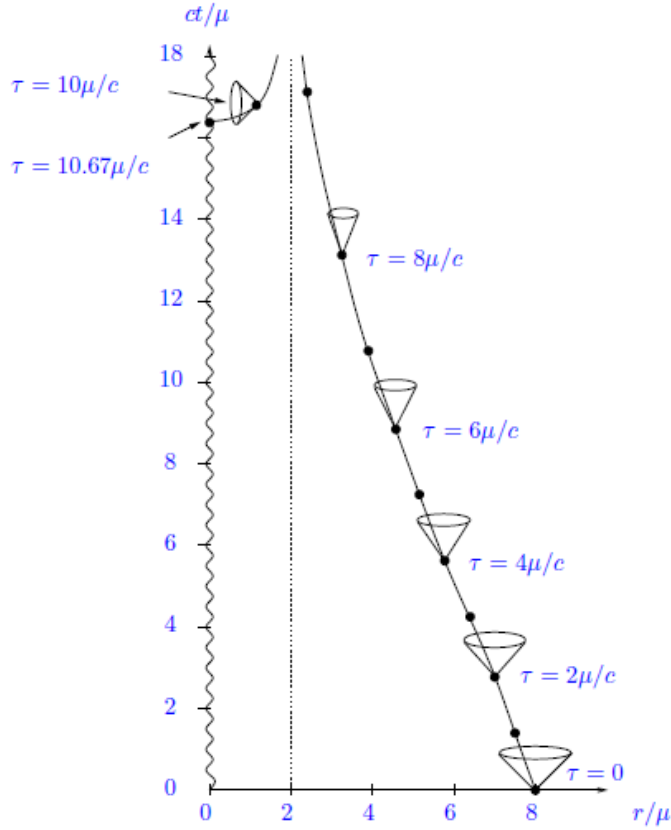


Figure 2: Trajectory of a radially-infalling particle released from rest at infinity. The dots correspond to unit intervals of  $c\tau/\mu$ , where  $\tau$  is the particle's proper time. We have taken  $\tau = t_0 = 0$  at  $r_0 = 8\mu$ . The particle reaches the singularity at  $r = 0$  at  $c\tau = 32\mu/3$ .

if it is emitted at  $r > 2\mu$ .

Since  $t$  is proper time for the distant observer (where the spacetime tends to Minkowski), they perceive that it takes an infinite amount of their proper time for the particle to reach  $r = 2\mu$  from any finite  $r > 2\mu$ .

The light signals emitted as  $r \rightarrow 2\mu$  are also infinitely redshifted when they reach the distant observer<sup>1</sup>.

As seen from the distant observer, the in-falling par-

<sup>1</sup>We shall work out the details later. For the moment, recall from Handout IX that the gravitational redshift between static observers becomes infinite as  $r \rightarrow 2\mu$ . Moreover, the signal is further redshifted for an in-falling emitter due to the Doppler effect.

title is never seen to cross  $r = 2\mu$ ; rather, it seems to hover there, forever becoming redder (and dimmer) and redder.

### 3 Eddington–Finkelstein coordinates

The time coordinate of the Schwarzschild solution is useful and physically meaningful as  $r \rightarrow \infty$  (as proper time experienced by a stationary observer there), but is inappropriate as  $r \rightarrow 2\mu$  and beyond.

Instead, let us try and construct coordinates that cover region I and the type-II region in its causal future without coordinate singularities.

We do this by adopting coordinates that are adapted to radially-infalling photons in such a way that their worldlines are continuous through  $r = 2\mu$ .

Recall that

$$ct = -r - 2\mu \ln \left| \frac{r}{2\mu} - 1 \right| + \text{const.} \quad (18)$$

for such photons.

Let us define a new time coordinate  $t'$  by

$$ct' \equiv ct + 2\mu \ln \left| \frac{r}{2\mu} - 1 \right|. \quad (19)$$

In terms of  $t'$  and  $r$ , ingoing radial null geodesics have

$$ct' = -r + \text{const.}, \quad (20)$$

and so are straight lines at  $45^\circ$  to the coordinate axes (as in Minkowski space).

For outgoing photons, recall that in the original coordinates

$$ct = r + 2\mu \ln \left| \frac{r}{2\mu} - 1 \right| + \text{const.}, \quad (21)$$

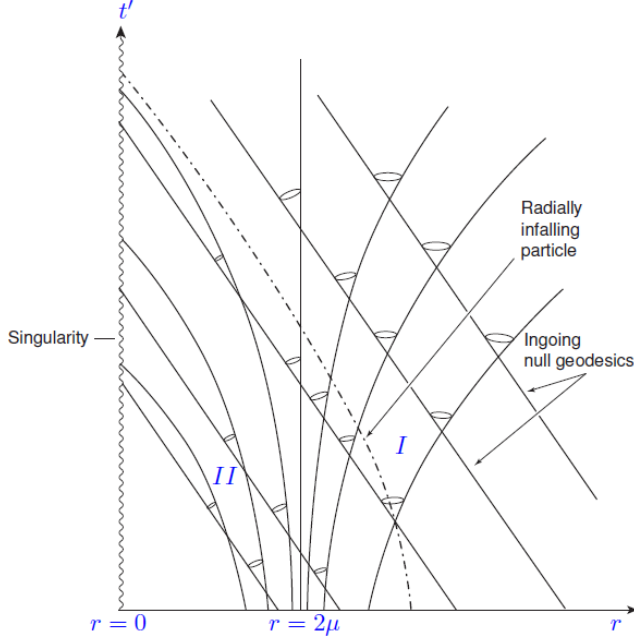


Figure 3: Lightcone structure of Schwarzschild spacetime in ingoing Eddington–Finkelstein coordinates. Ingoing radial null geodesics are straight lines at  $45^\circ$  to the coordinate axes. The path of a massive radially-infalling particle is also shown (dot-dashed line). Outgoing radial null geodesics in region I are still discontinuous at  $r = 2\mu$ .

so that

$$ct' = r + 4\mu \ln \left| \frac{r}{2\mu} - 1 \right| + \text{const.} \quad (22)$$

The spacetime diagram of these null geodesics and the associated forward lightcones are shown in Fig. 3.

The ingoing geodesics are now continuous at  $r = 2\mu$ , with the lightcones tilted over inwards there and in the black hole (region II).

To find the line element in these coordinates, we use

$$cdt' = cdt + \left( \frac{r}{2\mu} - 1 \right)^{-1} dr, \quad (23)$$

so that

$$ds^2 = \left(1 - \frac{2\mu}{r}\right) \left[ cdt' - \left(\frac{r}{2\mu} - 1\right)^{-1} dr \right]^2 - \left(1 - \frac{2\mu}{r}\right)^{-1} dr^2 - r^2 d\Omega^2. \quad (24)$$

Simplifying, we find

$$ds^2 = c^2 \left(1 - \frac{2\mu}{r}\right) dt'^2 - \frac{4\mu c}{r} dt' dr - \left(1 + \frac{2\mu}{r}\right) dr^2 - r^2 d\Omega^2. \quad (25)$$

This is no longer singular at  $r = 2\mu$  and, indeed, is regular for the whole range  $0 < r < \infty$ .

The time component of the metric does vanish at  $r = 2\mu$ , but this is not problematic since the metric is non-diagonal; the determinant is non-zero for  $r > 0$  and so the inverse metric exists.

The coordinates  $(t', r, \theta, \phi)$  are called *ingoing Eddington–Finkelstein coordinates* (sometimes *advanced* is used instead of ingoing).

### 3.1 Outgoing Eddington–Finkelstein coordinates

In ingoing Eddington–Finkelstein coordinates, the outgoing geodesics in region I are discontinuous at  $r = 2\mu$  (see Fig. 3).

They seem to originate from  $r = 2\mu$  at  $t' \rightarrow -\infty$  but, as in the original Schwarzschild coordinates, the affine parameter is finite there.

As we discussed earlier, this is because the causal *past* of region I is really another type-II region, but with the character of a white hole rather than a black hole.

The ingoing Eddington–Finkelstein coordinates do not cover this type-II region of spacetime.

However, we can always construct *outgoing Eddington–Finkelstein coordinates* that cover region I and the white hole in its causal past by taking

$$ct^* \equiv ct - 2\mu \ln \left| \frac{r}{2\mu} - 1 \right|. \quad (26)$$

In terms of  $r$  and  $t^*$ , the outgoing radial null geodesics have

$$ct^* = r + \text{const.}, \quad (27)$$

while the ingoing geodesics have

$$ct^* = -r - 4\mu \ln \left| \frac{r}{2\mu} - 1 \right| + \text{const.} \quad (28)$$

The outgoing null geodesics are now straight lines at  $45^\circ$  to the coordinate axes and the lightcones tip over to point *outwards* at  $r = 2\mu$  and within the white hole region  $r < 2\mu$ .

Of course, the ingoing geodesics are now discontinuous at  $r = 2\mu$ , with  $t^* \rightarrow \infty$  as  $r \rightarrow 2\mu$  but finite affine parameter.

These ingoing geodesics can be extended into the black hole region in the causal future of region I, but this region is not covered by the outgoing Eddington–Finkelstein coordinates.

To find the line element in these coordinates, we use

$$cdt^* = cdt - \left( \frac{r}{2\mu} - 1 \right)^{-1} dr, \quad (29)$$

so that

$$ds^2 = c^2 \left( 1 - \frac{2\mu}{r} \right) dt^{*2} + \frac{4\mu c}{r} dt^* dr - \left( 1 + \frac{2\mu}{r} \right) dr^2 - r^2 d\Omega^2. \quad (30)$$

This line element is also regular for the whole range  $0 < r < \infty$ .

The coordinates  $(t^*, r, \theta, \phi)$  are called *outgoing Eddington–Finkelstein coordinates* (sometimes *retarded* is used instead of outgoing).

As noted earlier, the global structure of Schwarzschild spacetime can be shown to consist of a black hole, a white hole and two type-I regions.

The ingoing and outgoing Eddington–Finkelstein coordinates each cover part of this, but it is possible to combine the two coordinate systems to form *Kruskal–Szekeres coordinates* that cover the global spacetime in a non-singular way.

We shall not need this here, but see, e.g., *Spacetime and Geometry: An Introduction to General Relativity* by Carroll for details if you are interested.

## 4 Formation of black holes

The Schwarzschild solution is a highly idealised configuration, with vanishing energy momentum everywhere except at the singularity at  $r = 0$ .

However, we believe that region I and the type-II region in its causal future are realised as the endpoint of stellar evolution of sufficiently massive stars.

After a star has expended its nuclear fuel, it will cool and lose pressure support causing it to contract under the influence of gravity.

If the star contracts to a radius smaller than  $2GM/c^2$ , it must inevitably collapse to form a singularity resulting in a black hole.



In practice, electron degeneracy pressure becomes important for a cold star that collapses to sufficient density, and this can hold the star up against gravitational collapse if the mass is below around  $1.4M_{\odot}$  (known as the *Chandrasekhar limit*).

Such *white dwarfs* are comparable in size to the Earth, but with the mass of the Sun.

For more massive stars, electron degeneracy pressure is insufficient to halt gravitational collapse.

In this case, the star collapses further until it reaches such densities that it becomes energetically favourable for electrons and protons to form (more massive) neutrons<sup>2</sup> and neutrinos forming a *neutron star*.

There is uncertainty over the equation of state for matter at the extreme densities found at the centre of a neutron star, but we think that the maximum mass of a neutron star is around  $4M_{\odot}$  and the radius would be around only 10 km.

A star more massive than this will inevitably collapse to form a black hole.

#### 4.1 Spherically-symmetric collapse of dust

As a toy-model for the formation of a black hole, consider the spherically-symmetric collapse of a cloud of pressure-free dust.

As there is no pressure support, the dust follows geodesics in spacetime.

---

<sup>2</sup>Although the neutron is more massive than the sum of the proton and electron masses, the Fermi energy of neutrons is lower than electrons at the same number density as their mass is so much higher.

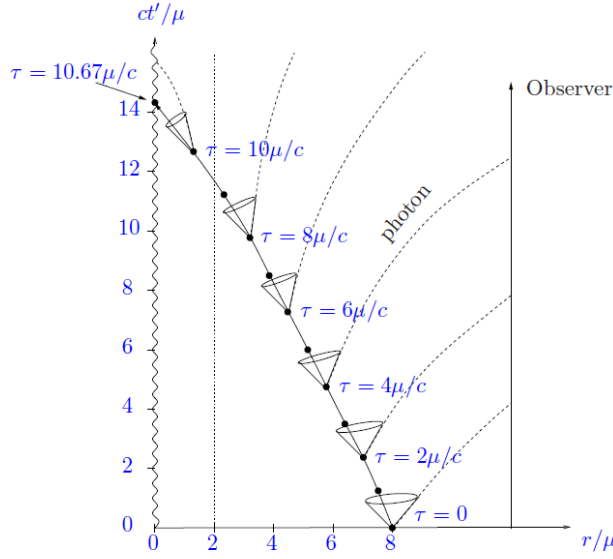


Figure 4: Collapse of the surface of a pressure-free dust cloud to form a black hole in ingoing Eddington–Finkelstein coordinates. The cloud’s surface started at rest at infinity, and we have chosen  $\tau = t' = 0$  at  $r = 8\mu$ .

By Birkhoff’s theorem, the spacetime *outside* the dust cloud will be described by the Schwarzschild solution, so we can treat the outside edge of the cloud as a massive particle free-falling radially in Schwarzschild spacetime.

For simplicity, we shall assume that the collapse starts from rest at infinity ( $k = 1$ ), and consider how the collapse appears to a stationary observer at rest at large radius  $r \gg \mu$ .

The trajectory of the edge of the dust cloud is shown in Eddington–Finkelstein coordinates in Fig. 4.

As discussed earlier, the distant observer will never see the surface of the dust cloud pass through  $r = 2\mu$ .

Light emitted after the surface crosses  $r = 2\mu$  will instead end up at the singularity at  $r = 0$ .

Moreover, the light is increasingly redshifted as  $r \rightarrow 2\mu$

so the frequency of light and the arrival rate of photons as measured by the distant observer fall to zero.

It follows that the distant observer sees the collapse slow down as  $r \rightarrow 2\mu$ , with the cloud becoming more and more red and more and dim.

Let us now work out some of the quantitative details.

Before the surface of the star crosses  $r = 2\mu$ , we can describe the collapse in terms of the standard Schwarzschild coordinates  $(t, r, \theta, \phi)$ .

Suppose the edge of the cloud emits a radially outgoing photon at coordinates  $(t_E, r_E)$ , which is received at  $(t_R, r_R)$  by the distant stationary observer.

Since these coordinates lie on an outgoing null geodesic, we have

$$ct_R - r_R - 2\mu \ln \left( \frac{r_R}{2\mu} - 1 \right) = ct_E - r_E - 2\mu \ln \left( \frac{r_E}{2\mu} - 1 \right). \quad (31)$$

The relation between  $ct_E$  and  $r_E$  is given by the path of the edge of the dust cloud; using Eq. (17), as  $r_E \rightarrow 2\mu$ , we have

$$ct_E = 2\mu \ln \left( \frac{\sqrt{r_E/2\mu} + 1}{\sqrt{r_E/2\mu} - 1} \right) + \text{const.} \quad (32)$$

Using this in Eq. (31), we have

$$\begin{aligned} ct_R &\rightarrow 2\mu \ln \left( \frac{\sqrt{r_E/2\mu} + 1}{\sqrt{r_E/2\mu} - 1} \right) - 2\mu \ln \left( \frac{r_E}{2\mu} - 1 \right) + \text{const.} \\ &= 2\mu \ln \left( \sqrt{r_E/2\mu} - 1 \right)^{-2} + \text{const.} \\ &\approx -4\mu \ln \left( \frac{r_E}{2\mu} - 1 \right) + \text{const.} \end{aligned} \quad (33)$$

It follows that

$$r_E(t_R) = 2\mu + a \exp(-ct_R/4\mu) , \quad (34)$$

where  $a$  is an unimportant constant.

We see that the radius the cloud has when observed at  $t_R$  approaches  $r = 2\mu$  exponentially with characteristic time  $4\mu/c$ .

For a Solar-mass cloud, the characteristic time is very short:  $4\mu/c = 2 \times 10^{-5}$  s.

We can also compute the redshift of the light from the surface.

We have

$$\frac{\nu_R}{\nu_E} = \frac{\mathbf{g}(\mathbf{p}_R, \mathbf{u}_R)}{\mathbf{g}(\mathbf{p}_E, \mathbf{u}_E)} , \quad (35)$$

where  $\mathbf{p}_E$  is the 4-momentum of a radial outgoing photon at emission at  $r_E$ , and similarly for  $\mathbf{p}_R$ , and  $\mathbf{u}_E$  is the 4-velocity of the edge of the dust cloud at  $r_E$  and  $\mathbf{u}_R$  is the 4-velocity of the distant observer.

We have

$$u_E^\mu = \left( (1 - 2\mu/r_E)^{-1/2}, -\sqrt{2\mu c^2/r_E}, 0, 0 \right) , \quad (36)$$

for the cloud starting from rest at infinity.

For the static observer, taking  $r \rightarrow \infty$ , we have

$$u_R^\mu = (1, 0, 0, 0) . \quad (37)$$

The 4-momentum of a radial outgoing photon is

$$p^\mu = \left( \frac{dt}{d\lambda}, \frac{dr}{d\lambda}, 0, 0 \right) = \frac{dt}{d\lambda} \left( 1, c \left( 1 - \frac{2\mu}{r} \right), 0, 0 \right) , \quad (38)$$

where we have used the null condition  $g_{\mu\nu}p^\mu p^\nu = 0$ .

As usual,

$$\frac{dt}{d\lambda} \left(1 - \frac{2\mu}{r}\right) = k, \quad (39)$$

where  $k$  is a constant.

It follows that

$$\nu_R = kc^2, \quad (40)$$

$$\nu_E = kc^2 \left(1 - \sqrt{\frac{2\mu}{r_E}}\right)^{-1}, \quad (41)$$

so

$$\frac{\nu_R}{\nu_E} = \left(1 - \sqrt{\frac{2\mu}{r_E}}\right). \quad (42)$$

Note that this tends to zero as  $r_E \rightarrow 2\mu$ .

Finally, using Eq. (34), we can write

$$\begin{aligned} \frac{\nu_R}{\nu_E} &\sim 1 - [1 + a \exp(-ct_R/4\mu)]^{-1/2} \\ &\sim \frac{1}{2}a \exp(-ct_R/4\mu), \end{aligned} \quad (43)$$

so the observed frequency decreases exponentially with characteristic decay time  $4\mu/c$ .